Synthesis and photoluminescence properties of photocatalysic materials with Sn doping

SHUXIA GAO[a], DEYI WANG[b*], PENG ZHANG [b], XIANJUN GUO[b], XIAOLONG ZHANG[b]
[a]*School of Opt-electric Information Technology, Yantai University, Yantai 264005, People's Republic of China*
[b]*School of Environment and Material Engineering, Yantai University, Yantai 264005, People's Republic of China*

In this paper, photocatalysic materials were synthesized by sol-gel method and showed the expected magnetic, photoluminesce and light absorbing mesoporous properties. Based on the experiment results, it is revealed that if the annealing temperature was at 550℃, the annealing time was 120min, the doping amount of Sn could reach 2.0at%. These produced samples were shown to have superior photoluminescence and UV-vis light absorbance. If the weight of template was set to 1.5g, for the obtained photocatalysic materials, their porous structures were mainly distributed within 1.2nm to 4.7nm and their specific surface areas were larger than 110m^2/g.

(Received September 7, 2016; accepted February 10, 2017)

Keywords: Three Dimensional Particle-Electrode, Process Condition, Structure, Optical Properties

1. Introduction

In recent years, micro-nanometer sized TiO_2 hollow structures nanomaterials have attracted a great deal of attention because of their high photo-catalytic activity, chemical stability, low cost, nontoxicity, low density, high surface area, superior surface permeability and large light-harvesting efficiencies[1–6]. Moreover, these materials can be widely applied in photoelectric devices, catalysis, drug delivery, chromatography separation and chemical reactors[7–12]. Various synthetic methods were explored to prepare hollow nanomaterials including self-assembly techniques, hydrothermal techniques, template-assisted techniques and chemically induced self-transformation[13–15]. Up to now, template-assisted synthetic method has been proved to be the most-applied and most-effective route to fabricate inorganic hollow structures. Titanium dioxide(TiO_2), as one of the most important transition-metal functional oxides, has attracted extensive attention during the past decades due to its superior physical and chemical properties and a wide variety of potential use in diverse fields such as solar energy conversion, environmental purification and water-treatment [16–18].

Herein, novel ZnO/SnO/SbO/Fe_2O_3/TiO_2 magnetic meso-porous luminescence materials were successfully fabricated using Sol-Gel-template method. It has been carefully researched that the effects, which was caused by the annealing conditions and the doping amount of zine and tin, on the structure, absorption property, light absorbing and luminesce property of the catalytic materials. Furthermore, the influence of amount of template on the distribution of porous and absorption capacity has been discussed in this paper.

2. Experimental procedures

The preparation of sol A: The butyl titanate was dissolved in Ethyl Alcohol. The solution was moved to a Kjeldahl flask.Certain amount of additives and different amounts of stannous chloride were added into the flask. This mixture was stirred slowly by a magnetic stirrer for 2 hours until all components were dissolved completely. During this process the temperature was constant at 40 ˚C.Then the transparent sol A was obtained and moved to a dry beaker.

The preparation of sol B: Ethyl Alcohol and Acetic acid were mixed up together and moved to a Kjeldahl flask. This solution was stirred by a magnetic stirrer and the temperature was kept in 40˚C. At the same time, sol A was dropped into the solution at the speed of 1 drop per second. After this, Macrogol 4000 was added into the flask. When the above solution was become clear, concentrated nitric acid was added slowly at the speed of 1 drop per 30 seconds. Then the PH value of the solution was adjusted to 3.0. This mixture was stirred continually for 3 hours, then sol B was gained which was transparent, light yellow.

Sol B was aged for 12 hours at the room temperature. Then sol B was put into a drying-oven for 240 minutes at the constant temperature 80˚C, then sol B was changed to semi-transparent gel. Subsequently, the temperature of drying-oven was increased to 105˚C for another 240

minutes. Then sol B was become into solid powder and grounded in a star shape grinder for 30 minutes

The solid powder was moved into a crucible which was inside of a tube furnace. The temperature and time of anneal were stetted differently forgetting different samples. The sample was cooled down to room temperature naturally.

The XRD, UV-vis Absorption Spectrum, PL spectrum and BET surface area analyser were used to analyses and characterize the structure and property of the samples.

3. Results and discussion

3.1. Effects of Sn-doped concentration on the structure and optical properties of three dimensional particle-electrode

In this experiment, the contents of Ti, Sb, Zn, and Fe were constant, the doping amount of Sn was changed, and the details were shown as 0.5%,1%,2%,3%,and 4%(percentage of Sn to Ti). According to the method which was described above, the obtained dry solid powder was put into a tube furnace, the annealing temperature was at 550˚C and the annealing time was set in 120 minutes.

3.1.1. Structure characterizations

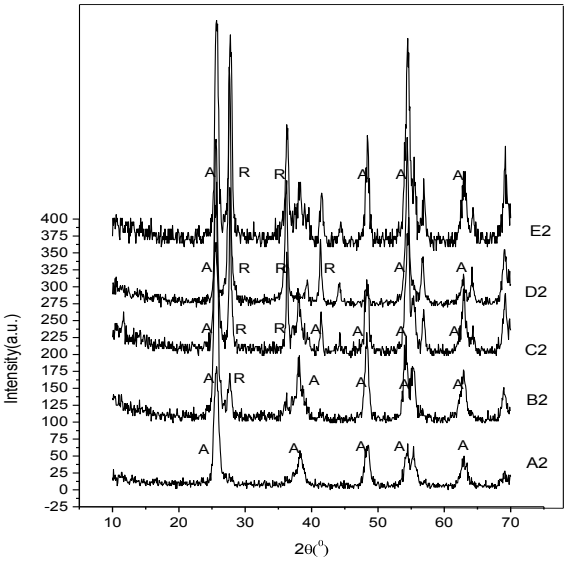

Fig. 1. XRD Spectrum of the samples with different Sn contents (A2:0.5% , B2:1% , C2:2% , D2:3% , E2:4%)

Fig. 1 shows the XRD spectrum of Zn/Fe/Sn/Sb-TiO_2 3D Particle Electrode with different doping amounts of Sn. As shown in Fig. 1, the crystal structure of samples changed as the doping amount of Sn increased. When the doping amount of Sn was 0.5%, the main diffraction peaks of samples were all attributed to the crystal surface 101, 004, 200, 211 and 204 of anatase structure. When the content of Sn was increased to 1% ~2%, the diffraction peak of rutile phase started to appear, but the dominated structure was still anatase structure. When the content of Sn was more than 3%, the crystal structure of samples deformed dramatically, the intensity of diffraction peak of rutile enhanced and some unrecognized peaks appeared. In this regard, it could be determined tentatively that the doping amount of Sn should be lower than 2%.

3.1.2. Optical properties

3.1.2.1 PL Spectrum

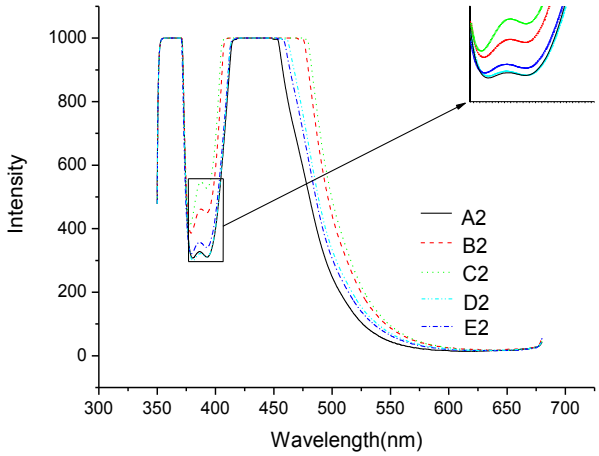

Fig. 2. PL Spectrum of samples with different Sn contents

From Fig. 2, it was revealed that the samples of the 2nd Group all had strong UV luminescence peaks when the wavelength was between 350nm-375nm, when the wavelength was approximately equal to 450nm, the photo peaks appeared in visible light region. When the content of Sn was between 1% and 2%, the range of wavelength of luminescence peak at visible region became wider which was about 400nm-500nm. When the content of Sn was less than 1% or more than 2%, the range of wavelength of luminescence became smaller. In addition, when the content of Sn ranged from1% to 2%, there was a small luminescence peak during the wavelength was between 375nm and 410nm for all samples; however the peaks of sample B2 and C2 were much higher than the other samples. In terms of the change trend of PL spectrum, it could be determined initially that the proper range of Sn content was 1% to 2%.

3.1.2.2. UV-vis Absorption spectrum

Based on the Fig. 3, when the Sn content was lower than 2%, the absorbance increased as the content of Sn increased when the wavelength was 200nm to 700nm.On the contrary, when the doping amount of Sn was higher than 2%, the absorbance decreased as the content of Sn

increased when the wavelength was 200 to 700nm. The absorbance of these samples that contained 2% Sn content were all excellent during the wavelength was between 200 to 700nm.

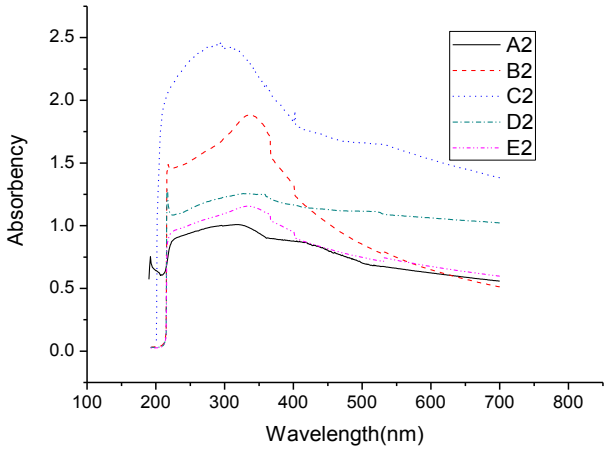

Fig. 3. UV-vis Spectrum of samples with different zine contents

3.2 Influences of annealing temperature and time

3.2.1. The influence of annealing temperature

The samples were annealed at 450˚C, 550˚C, 600˚C, 650˚C and 700˚C for 120 min respectively and then cooled down to room temperature.

When the temperature was higher than 600˚C, the intensity of diffraction peak of anatase structure reduced, the intensity of diffraction peak of rutile structure increased. Therefore, the annealing temperature should be lower than 600˚C.

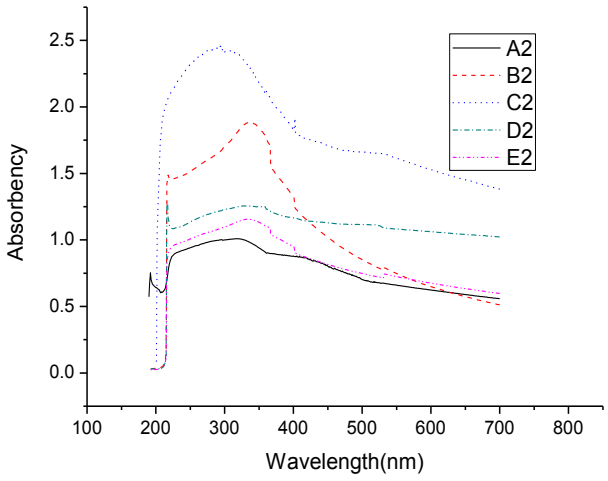

Fig. 4. XRD spectrum of samples in different annealing temperature

3.2.2. Influences of annealing time

The samples were annealed at 550˚C for 90min, 120 min, 150 min and 180 min, respectively and then cooled down to room temperature.

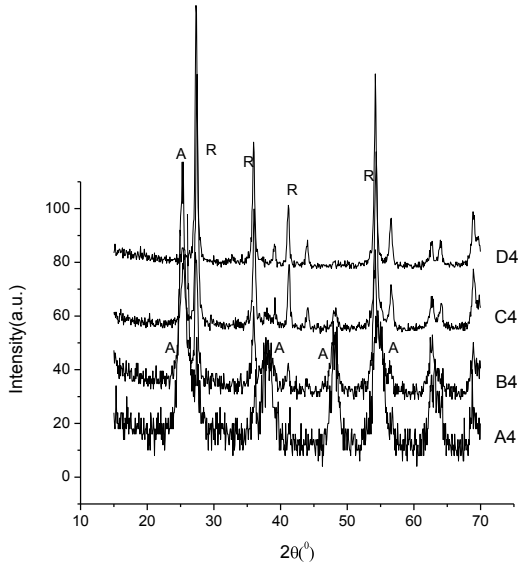

Fig. 5. XRD spectrum of samples with different annealing time

According to Fig. 5, if the annealing time was 90 minutes, there was only one diffraction peak of anatase structure, but the peak height was low, the peak FWHM was wide. This indicated that short annealing time was not good at the growth of crystal. When the annealing time was increased to 120 minutes, the main diffraction peak was anatase structure peak, the intensity of diffraction was strong, the peak FWHM became narrow. This indicated that this annealing time was conductive to the growth of crystal. When the annealing time was more than 150 minutes, the intensity of diffraction peak of anatase structure decreased, on the contrary, the intensity of rutile structure increased. Therefore, the annealing time should not be more than 120 minutes.

3.3. Influences of the amount of template on the absorbance of 3D Particle Electrode

The amount of each element in the preparation of sol A and sol B was unchanged, as Zn4.0at%, Sb1.0at%, Sn2.0at% and Fe2.5at%, respectively. The amount of template F127 was 0g, 0.5g, 1.0g, 1.5g, 2.0g, 2.5g, 3.0g and 3.5g.

From Fig. 6, it can be concluded that the usage of template could improve the absorbance and specific surface area of electrode significantly. When the amount of template was lower than 1.5g, the specific surface area increased significantly as the amount of template increased, the peak width of pore-diameter distribution curve

decreased significantly as the amount of template increased. When the amount of template was 1.5g, the corresponding specific surface area was 110m^2/g, the peak width of the pore-diameter distribution curve reduced to 1.2-4.7nm. According to the calculation, the volume of pore, which was range at 1.2 to 4.7nm, was 84% of the total pore volume of the sample, it indicated that the samples that were made under this condition had excellent pore-diameter distribution. When the amount of template was more than 1.5g, the specific surface area of samples decreased as the amount of template increased, the peak width increased obviously as the amount of template increased. Therefore there was an optimum amount of template. Overloaded template would affect the pore-diameter distribution of the samples significantly, the quantity of the pore-diameter which was more than 10nm increased distinctly. Therefore, when the amount of template was more than 1.5g, the specific surface area of samples decreased significantly as the template increased rather than increasing.

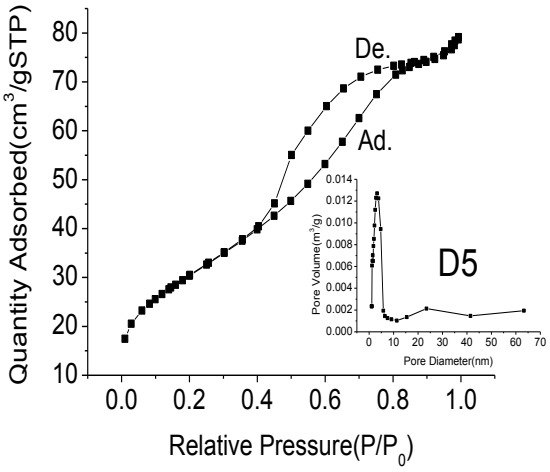

Fig. 6. Porous distribution curve and adsorption isotherm of the sample (1.5g template)

4. Conclusions

The novel ZnO/SnO/SbO/Fe_2O_3/TiO_2 magnetic meso-porous photo-catalytic materials were successfully fabricated by using Sol-Gel-template method. This experiment included the detailed investigation about the influence on the catalytic materials caused by changing annealing conditions and the doping amount of zine and tin. In addition, it also focused on the relationship of the porous distribution, absorption capacity and the amount of template.

The doping amount of Sn was 2.0at%, obtained samples has excellent luminesce property. For the wavelength is in the range of 200nm to 700nm, the obtained samples has superior light absorbance. Excellent light absorbance is essential for a photocatalystic material to have good performance. Under the condition that the template was set to 1.5g, the obtained photocatalysic materials, indicated that their porous mainly distributed within 1.2nm to 4.7nm and their specific surface areas were larger than 110m^2/g, and had excellent absorption properties.

Acknowledgements

The authors wish to acknowledge the financial support of the National Natural Science Foundation of China (no. 41271506) and the Science and Technology Development Project of Yantai(no.2014ZH076) .

References

[1] Xiaoyan Zhang, Yujun Sun, Xiaoli Cui, Zhiyu Jiang, International Journal of Hydrogen Energy **37** (2), 1356 (2012).
[2] Qian Zhang, Wei Li, Shouxin Liu, Powder Technology **212**(1), 145 (2011)
[3] Kwangjin An, Soon Gu Kwon, Mihyun Park, Hyon Bin Na, Sung-Il Baik, Jung Ho Yu, Dokyoon Kim, Jae Sung Son, Young Woon Kim, In Chan Song, Woo Kyung Moon, Hyun Min Park, Taeghwan Hyeon, Nano Letters **8**, 4252 (2008)
[4] Hualan Zhou, Zhong Zou, Sha Wu, Fangzhou Ge, Ying Li, Wenjian Shi, Material Letters **65**(6), 1034 (2011).
[5] Jiaguo Yu, Shengwei Liu, Huogen Yu, Journal of Catalysis **249**(1), 59 (2007).
[6] Sihui Zhan, Jiangyao Yang, Yu Liu, Nan Wang, Jingjing Dai, Hongbing Yu, Xichao Gao, Yi Li, Journal of Colloid and Interface Science **355**(2), 328 (2011).
[7] Qinghang He, Zhenxi Zhang, Jianwen Xiong, Yuying Xiong, Hua Xiao, Optical Materials **31**(2), 380 (2008).
[8] Penghui Zhao, Weilong Li, Gang Wang, Baozhi Yu, Xiaojun Li,Jintao Bai,Zhaoyu Ren, Journal of Alloys and Compounds. **604**, 87 (2014).
[9] Zhengying Gu, Xiangdong Gao, Xiaomin Li, Zhengwu Jiang, Yudi Huang, Journal of Alloys and Compounds. **590**, 33 (2014).
[10] Xue Bai, Xiaoyuan Zhang, Zulin Hua, Wenqiang Ma, Zhangyan Dai, Xin Huang, Haixin Gu, Journal of Alloys and Compounds, **599,** 10 (2014).
[11] Guidong Yang, Zifeng Yan, Tiancun Xiao, Bolun Yang, Journal of Alloys and Compounds **580,** 15 (2013).

[12] Mukhtar Ahmad, Ihsan Ali, R. Grössinger, M. Kriegisch, F. Kubel, M. U. Rana, Journal of Alloys and Compounds **579**, 57 (2013).
[13] Xujie Lu, Fuqiang Huang, Jianjun Wu, Shangjun Ding, Fangfang Xu, ACS Applied Materials Interfaces **3**(2), 566 (2011).
[14] Jiaguo Yu, Xiaoxiao Yu, Environmental Science Technology **42**(13), 4902 (2008)
[15] Xiaoning Wang, Baibiao Huang, Zeyan Wang, Xiaoyan Qin, Xiaoyang Zhang, Ying Dai, Myung-Hwan Whangbo, Chemistry European Journal **16**(24), 7106 (2010).
[16] Bin Liu, Eray S. Aydil, Journal of the American Chemical Society **131**(11), 3985 (2009).
[17] Yunqian Dai, Claire M. Cobley, Jie Zeng, Yueming Sun, Younan Xia, Nano Letters. **9**(6), 2455 (2009).
[18] Haifeng Lin, Liping Li, Minglei Zhao, Xinsong Huang, Xiaomei Chen, Guangshe Li, Richeng Yu, Journal of the American Chemical Society **134**(20), 8328 (2012).

*Corresponding author: wangdy107@163.com